

General Disclaimer

One or more of the Following Statements may affect this Document

- This document has been reproduced from the best copy furnished by the organizational source. It is being released in the interest of making available as much information as possible.
- This document may contain data, which exceeds the sheet parameters. It was furnished in this condition by the organizational source and is the best copy available.
- This document may contain tone-on-tone or color graphs, charts and/or pictures, which have been reproduced in black and white.
- This document is paginated as submitted by the original source.
- Portions of this document are not fully legible due to the historical nature of some of the material. However, it is the best reproduction available from the original submission.

NASA
Technical Memorandum 83488

AVRADCOM
Technical Report 83-C-10

(NASA-TM-83488) SOME INELASTIC EFFECTS OF
THERMAL CYCLING ON YTTRIA-STABILIZED
ZIRCONIA (NASA) 13 p HC A02/MF A01 CSCL 20D

N84-16492

Unclas
G3/34 18121

Some Inelastic Effects of Thermal Cycling on Yttria-Stabilized Zirconia



Robert C. Hendricks and G. McDonald
Lewis Research Center
Cleveland, Ohio

and

Robert C. Bill
Propulsion Laboratory
AVRADCOM Research and Technology Laboratories
Lewis Research Center
Cleveland, Ohio

Presented at
Eighty-fourth Annual Meeting and Exposition of the
American Ceramic Society
Cincinnati, Ohio, May 2-5, 1982

NASA



SOME INELASTIC EFFECTS OF THERMAL CYCLING ON YTTRIA-STABILIZED ZIRCONIA

Robert C. Hendricks and G. McDonald

National Aeronautics and Space Administration
Lewis Research Center
Cleveland, Ohio

and

Robert C. Bill

Propulsion Laboratory
AVRADCOM Research and Technology Laboratories
Lewis Research Center
Cleveland, Ohio

ABSTRACT

An analysis has been developed which relates the effects of inelastic behavior of yttria-stabilized zirconia (YSZ) materials. The results show these materials to be sensitive to small changes in temperature and are supported by measurements of inelastic behavior in disc and bar specimens at temperatures as low as 1010° C (1850° F). At higher thermomechanical loadings, the test specimens can deform to strains above 1 percent.

INTRODUCTION

It has previously been determined that stresses in layered ceramics, such as applied to seals and other components, are sensitive to both the temperature and heating rates (ref. 1) related to adhesion/cohesion effects (ref. 2), coating crack development and life (ref. 3), and inelastic material behavior (ref. 4). There are wide variations in both the adhesive/cohesive strength of a 0.38-mm yttria-stabilized zirconia (YSZ) plasma-sprayed ceramics (ref. 5) and the number of cycles to failure when subjected to a Mach 0.3 burner flame. Moreover, when YSZ is plasma-sprayed onto a metallic substrate and heated in a Mach 0.3 flame between 930° and 1040° C, extremely large decreases in specimen life are found at the higher temperatures (ref. 6). At the higher temperatures some process is occurring which accelerates the accumulation of sufficient stress to spall the ceramic from the metallic substrate.

Spalling is the mode of most obvious failure in plasma-sprayed ceramic coatings. The serious consequences of spalling include direct exposure of structural metal substrates to the high temperature turbine gas environment. Factors that promote spalling include thermal stress loading of the ceramic bondcoat interface, oxidative or corrosive degradation of the ceramic bondcoat interface, and development of internal stresses within the porous ceramic coating due to condensation of combination products in the pores.

Since there is a large difference in thermal expansion of the ceramic layer on a metallic substrate under even isothermal conditions, the metal, at elevated temperatures, is stressing the ceramic in tension. When maintained

at temperature, the ceramic may undergo inelastic behavior and, on subsequent cooldown, the ceramic would be compressed. This compressive load may be sufficient to spall the ceramic directly on cooldown, or it may be sufficient, when combined with compressive stresses from subsequent heatup cycles, to cause eventual spalling.

This paper describes some results obtained from the experimental measurements of inelastic behavior of YSZ as applied to plasma-sprayed ceramics.

SYMBOLS

b	load effect on thermal creep
F	transverse load
P	load
T	temperature
ϵ_j	inelastic strain
σ	stress
τ	time
ν	Poisson ratio

Subscripts:

calc	calculated
exp	experimental
0	reference

APPARATUS AND PROCEDURE

Tests were conducted on YSZ disc and bar samples (fig. 1). The 0.38-mm (0.015-in.) thick YSZ disc samples were 25 mm in diameter, supported on a tube holder, and loaded by a ball-in-cage system with additional weights added to the cage. The bar samples consisted of 1.5 by 13 by 140-mm stainless steel flat stock and were plasma-sprayed on both sides with 0.13 mm of NiCrAlY and 0.38 mm of YSZ. The edges were essentially uncoated. The bar specimens, supported on a reinforced U-channel, were loaded by round stock secured in position by a wire loop.

In both types of tests, the samples were statically transverse-loaded and heated in an argon-flooded furnace for predetermined times and temperatures. Photographs of typical disc and bar specimens appear in figure 2 and will be discussed next.

RESULTS AND DISCUSSION

In an effort to determine some inelastic behavior in YSZ materials, several static furnace experiments were conducted, the results of which are presented in figure 2 and the tables.

While the disc specimens (fig. 2(a)) represent a 'homogeneous' material, the sprayed bar specimens (fig. 2(b)) represent a composite material with concave and convex surfaces in compression and tension, respectively, with defor-

mation controlled by the substrate under applied load. At 1177° C and 210 gm loading, severe deformation of the bar specimen can occur. On the tension side, a strain relieved debonded surface projected the ceramic layer 0.2 mm beyond the substrate (fig. 2(c)). In figure 2(d), the ceramic on the compression and tension sides of the bar (fig. 2(c)) has been removed to demonstrate the inelastic behavior. The debonding crack on the tension side is shown more clearly in figure 2(d). The tension surface is fragile and possesses a multiplicity of small cracks as compared to the compression surface.

It is apparent from the data of these tests (table II and figs. 2(c) and (d)) that the NiCrAlY bondcoat material retains sufficient strength to stress the YSZ on surfaces of concave or convex curvature.

The inelastic deformation of the region beneath the load for disc and bar samples is given in tables I and II. For the disc, the composite strain is approximated as the ratio of deformed to undeformed surface area where the deformed surface is represented as a cone. The calculated values of disc strain are estimated using equations (1) and (2), as developed in the appendix, for the inelastic contribution and those of reference 9 for the elastic contribution.

$$\epsilon_i = (\tau/\tau_0)^{0.55} \quad (1)$$

$$\epsilon_i = 4.35 \times 10^{-3} \sigma^{1.07} \tau^{0.55} e^{-1230/\Delta T} \quad (2)$$

It is assumed that the applied stress due to transverse load remains constant and the concentrated and uniform loads are related as

$$F = \left(\frac{5 + \nu}{3 + \nu} \right) \frac{\pi d^2}{16} P \quad (3)$$

For most data, the experimental and calculated values are of the same order of magnitude. For the point (1010° C, 173.4 gm), the heating time is in question and has not been resolved.

Figure 3 presents a qualitative comparison of strains produced on transverse-loaded disc specimens (fig. 2(a) and table I) with those for uniaxial strains produced by compressive loading of cylindrical shells (ref. 4) for selected temperatures and loadings. The solid curves represent data of reference 4. The solid symbols represent data of this study and the open symbols and the dashed curves are estimated from equations (1) and (2). Here σ_{max} was assumed as 27 MPa. The 1-percent strain axis through the figure is important as it represents various values of τ_0 (eq. (1)).

The evidence relating to inelastic behavior does indicate that heating history at elevated temperature can significantly influence life.

ANALYSIS

Since there exists several comprehensive data sets for cylindrical specimens (13 mm diam), the basic analysis for inelastic behavior will be for a cylinder.

The computer codes SINDA and FEATS (refs. 7 and 8) were used to analyze the transient thermomechanical load cycle associated with a multimaterial-sprayed rod subjected to a Mach 0.3 Jet-A air burner flame (ref. 1). For this elastic model, the effects of inelastic behavior were simulated using the enforced axial displacement constraint which, per unit length, becomes equivalent to axial strain. Under such conditions, the compressive stress increases significantly which in turn produces higher circumferential and radial stresses. Assuming the materials can withstand these strains, the development of radial stress in a YSZ-sprayed rod specimen as a function of initial axial strain is illustrated in figure 4 for the initial phase of the heating transient.

For a radial stress or an average adhesive/cohesive stress of 9 MPa, the initial axial strain is approximately 0.35 percent. While a direct comparison for inelastic behavior of the rod at 1040° C (1900° F) under the prescribed experimental thermomechanical loading is unavailable, an estimate for inelastic behavior can be made using equations (1) and (2). Assuming a thermomechanical loading of 1040° C and 24.1 MPa, 1.19E4 or 3980 3-min temperature cycles would cause an inelastic strain of 0.35 percent. Experimentally, the average life is 1330 cycles (ref. 5) or about one-third of the estimated value of 3980.

To illustrate the sensitivity of these results to temperature at a thermomechanical loading of 1060° C and 24.1 MPa, 1620 min or 540 3-min cycles are required to produce a 0.35-percent strain.

It is evident that more analytical and experimental results are necessary to adequately resolve the problems.

SUMMARY

Experimental tests and an analysis of cyclic heating life of zirconia-sprayed ($ZrO_2-Y_2O_3/nCrAlY$) specimens have demonstrated that applied thermal rate and temperature level are important parameters in thermal cycle life of the ceramic.

A YSZ specimen which can withstand the rate at which heat is applied (thermal shock) then becomes subjected to higher temperature effects. Inelastic behavior (creep) can increase strains on the ceramic layer, thereby degrading the specimen's ability to withstand thermal shock or the directly applied compressive load. The magnitude of the inelastic effects are sensitive to small changes in temperature.

These results are supported by measurements of inelastic deformation of transversely loaded plasma-sprayed disc and plasma-sprayed bar specimens to temperatures as low as 1010° C (1850° F). At higher thermomechanical loads (e.g., a disc specimen at 1066° C with 173 gm load), the observed strains were above 1 percent.

APPENDIX - SEMI-EMPIRICAL APPROXIMATIONS FOR CREEP BEHAVIOR

The details and results of a variety of creep tests with YSZ (ref. 4) are not yet fully available. In brief, YSZ was plasma-sprayed onto aluminum tubes which were NaOH-leached to provide the YSZ cylindrical shell which was compressive-loaded at different temperatures and loads.

The form selected to represent these data is

$$100 \epsilon_i = (\tau/\tau_0)^p \quad (A1)$$

where τ_0 is the time (in min) at temperature and while $0.5 < p < 0.7$, a value of 0.55 was selected.

An approximate relationship

$$\log_{10} \tau_0 = \frac{\left(\frac{100}{T - T_0} \right) - b}{0.103} \quad (A2)$$

can be established where τ_0 is the time to induce a creep strain of 1 percent at temperature T , T_0 is a reference temperature set at 1173 K (900° C), and b represents the effect of applied loading on the YSZ cylinder (fig. 5).

The effect of applied load must be greater than zero but less than the rupture loading; however, the nonlinearity and temperature dependence which enters the relation is not clear. The parameter b is approximated by

$$b = 0.1 + 0.2 \log_{10}(P/P_0) \quad (A3)$$

where P is the applied loading and P_0 is a reference loading of 6.9 MPa (1000 psi).

Equations (A2) and (A3) can be combined to give

$$\tau_0^{-0.55} = 3.42(\sigma/\sigma_0)^{1.068} e^{-[1230/(T-T_0)]} \quad (A4)$$

and equation (A1) rewritten as

$$\epsilon_i = 4.35 \times 10^{-3} \sigma^{1.068} \tau_0^{0.55} e^{-1230/\Delta T} \quad (A5)$$

with creep rate given as

$$\dot{\epsilon}_i = 2.39 \times 10^{-3} \sigma^{1.068} \tau_0^{-0.45} e^{-1230/\Delta T} \quad (A6)$$

REFERENCES

1. G. McDonald and R. C. Hendricks, "Effect of Thermal Cycling on ZrO₂-Y₂O₃ Thermal Barrier Coatings," Thin Solid Films **73**, 491-496 (1980).
2. S. R. Levine, "Adhesive-Cohesive Strength of a ZrO₂.1-2 w/o Y₂O₃/NiCrAlY Thermal Barrier Coatings," NASA TM-73792, 1978.
3. C. A. Andersson, R. J. Bratton, S. K. Lau, S. Y. Lee, J. Allen, K. E. Munsen, and K. L. Rieke, "Advanced ceramic coating development for industrial/utility gas turbine applications," NASA-CR-165619, February 1982 (Westinghouse Electric Corp., DEN3-110).
4. R. F. Firestone, W. R. Logan, and J. W. Adams, "Creep plasma sprayed zirconia," NASA-CR-167868, November 1982 (IIT Research Institute, IITRI-M06071-20).
5. R. C. Hendricks and G. McDonald, "Assessment of Variations in Thermal Cycle Life Data of Thermal-Barrier Coated Rods," NASA TM-81743, 1981.
6. R. C. Hendricks, G. McDonald, and N. J. Poolos, "Prolonging Thermal Barrier Coated Specimen Life By Effective Thermal Management," NASA TM-81742, 1981.
7. G. Cowgill; P. Manos, NASA LeRC, Private Communication, SINDA PROGRAM.
8. J. A. Swanson, "FEATS - A Computer Program for the Finite Element Thermal Stress Analysis of Plane of Axisymmetric Solids," WANL-TME-1888, Westinghouse Electric Corp., Pittsburgh, PA, 1968.
9. Raymond J. Roark, Formulas for Stress and Strain, McGraw-Hill, New York, 3rd Ed., 1954.

**ORIGINAL PAGE 3
OF POOR QUALITY**

**TABLE I. - INELASTIC BEHAVIOR OF YSZ DISK SPECIMENS HEATED
IN AN ARGON-FLOODED FURNACE**

Temperature, °C	Time, min	Load, gm	Deflection, mm	Percent-strain		Symbol
				exp	calc ^a	
1010	5400	97.4	0.12	0.005	0.0045	◇
1010	5760	173.4	1.4	.6	.009	△
1066	5400	97.4	.9	.24	.2	○
1066	5400	173.4	1.65	.84	.36	▽
1121	5400	97.4	3.4	3.5	1.23	□

^aEq. (1).

**TABLE II. - INELASTIC BEHAVIOR OF
YSZ-NiCrAlY SUBSTRATE BAR
SPECIMENS IN AN ARGON-
FLOODED FURNACE**

[Specimen weight, 41.1 gms;
heating time, 24 hr.]

Temperature		Load, gm	Deflection	
°C	°F		mm	in.
1066	1950	64.2	1.8	0.07
		133.6	3.8	.15
		210.4	6.6	.26
1121	2050	62.4	2.0	.08
		133.6	4.3	.17
		210.4	7.4	.29
1177	2150	210.4	12.2	.48

ORIGINAL PAGE 13
OF POOR QUALITY

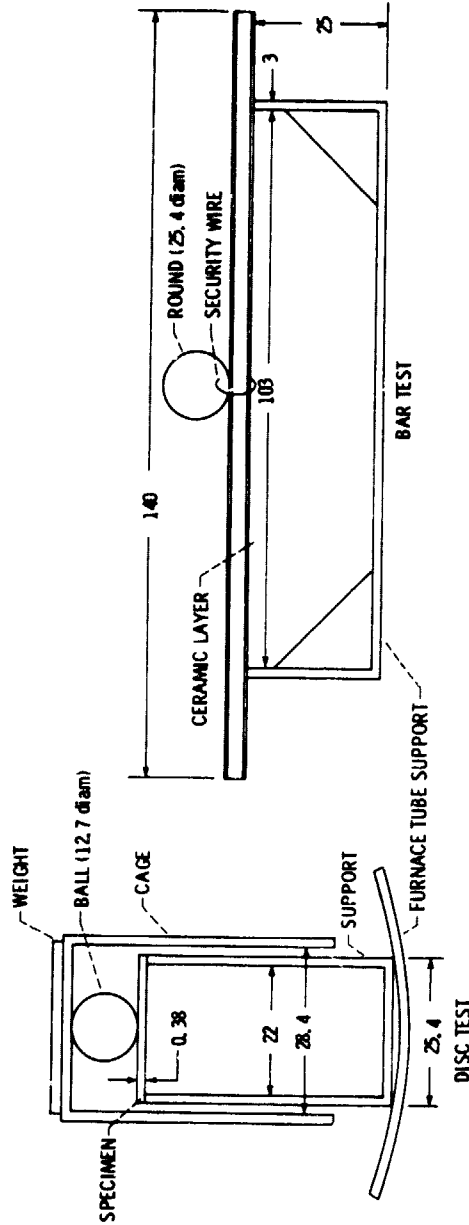
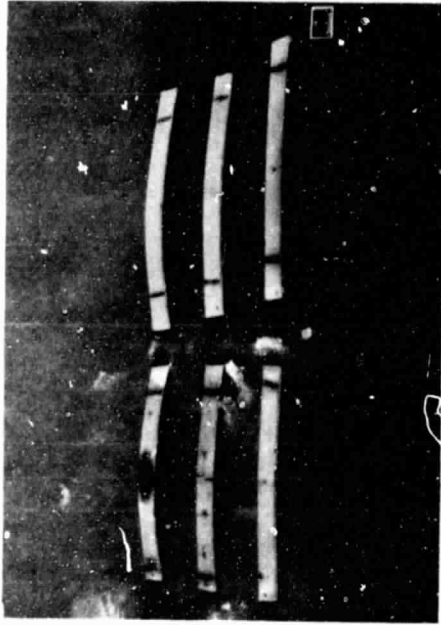
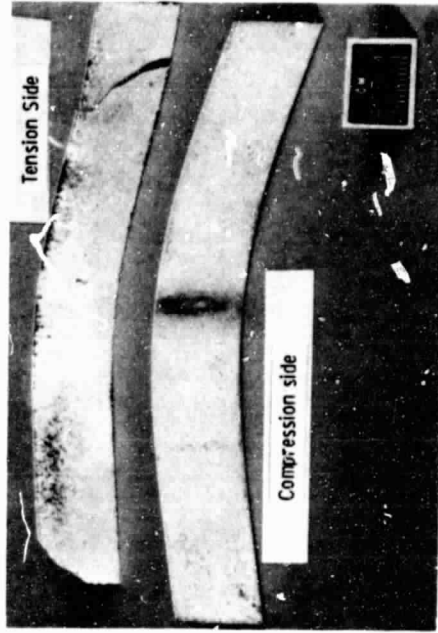


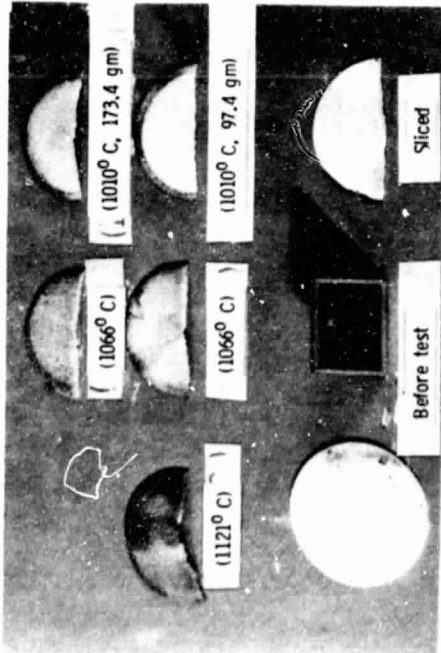
Figure 1. - Schematic of test apparatus for furnace testing disc and bar specimens (dimensions in mm).



(b) Zirconia-sprayed bar specimens.

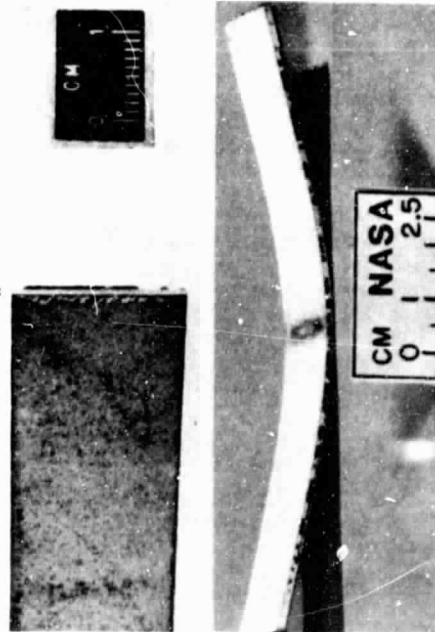


(d) Inelastic ceramic behavior.
(1177° C, 210 gm)



(a) Disc specimens.

→ 0.2 mm



(c) Inelastic zirconia-sprayed bar behavior.
(1177° C, 210 gm)

Figure 2 - Photographs of test specimens.

ORIGINAL PAGE IS
OF POOR QUALITY

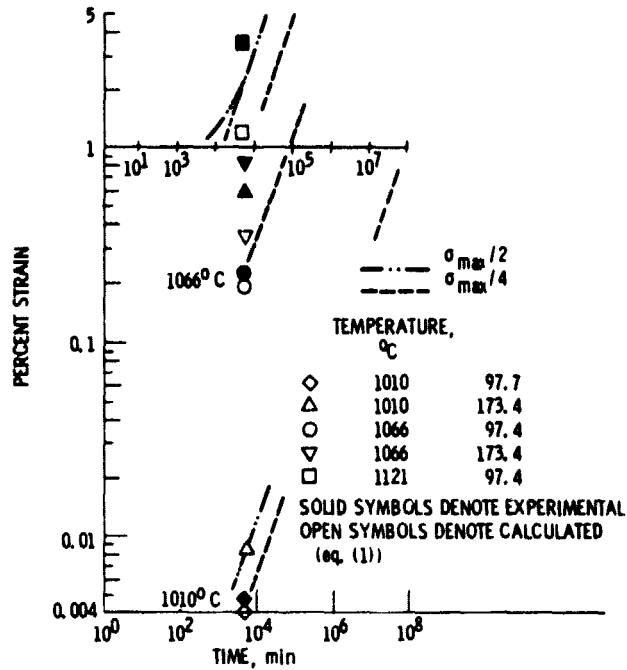


Figure 3. - Comparison of thermal creep results for transverse-loaded disc specimens and axial compression-loaded cylindrical shells (ref. 4).

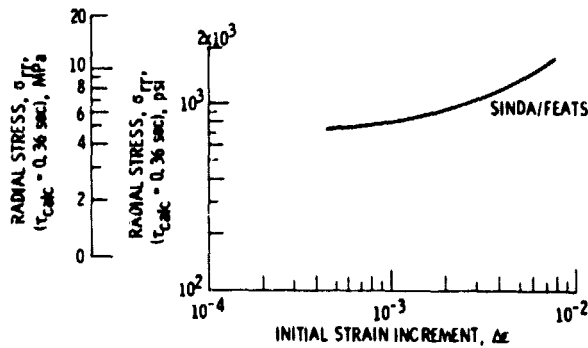


Figure 4. - Stresses in YSZ-sprayed rod specimen with initial axial displacements.

ORIGINAL PAGE 19
OF POOR QUALITY

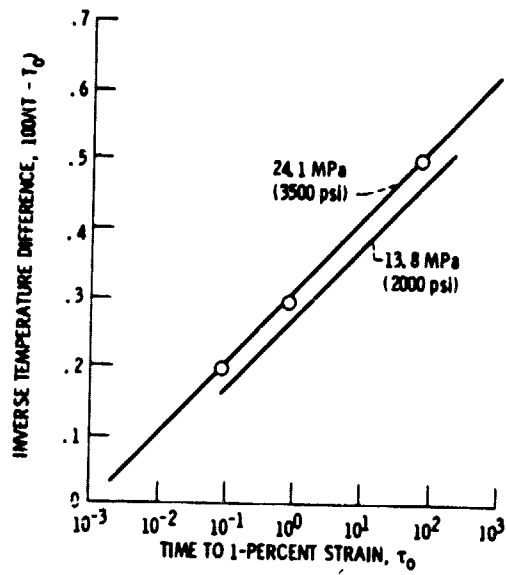


Figure 5. - Variation of compressive creep with thermomechanical loading (data from ref. 4).